THE LARGE DEFORMATION ELASTIC RESPONSE OF WOVEN KEVLAR FABRIC*

SAND--91-0653C
DE91 010582

by

William E. Warren, Fellow ASME
Sandia National Laboratories
Albuquerque, NM 87185

ABSTRACT

The large deformation elastic response of a plane woven Kevlar fabric is investigated analytically and experimentally. The analysis assumes the undeformed geometry to be a sequence of interlaced arcs of circles which reverse at each yarn midpoint, and each yarn is modeled as an extensible elastica subject to certain compatibility conditions. Deflection-force relations for the fabric are determined in terms of the initial weave geometry and the elastic properties of the individual yarns. The theoretical results agree well with the results of experiments performed on a fabric woven from 400 denier Kevlar yarns under conditions of uniaxial loading in both warp and fill directions.

* This work performed at Sandia National Laboratories and supported by the U. S. Department of Energy under contract # DE-AC04-76DP00789.

INTRODUCTION

Woven Kevlar fabrics exhibit a number of beneficial mechanical properties which include strength, flexibility, and relatively low density. Fabrics are used, for example, in parachutes and bullet-proof vests, and they are often used as the reinforcement in individual laminates of a composite material. The desire to engineer or design Kevlar fabrics for specific applications has stimulated interest in the development of theoretical models which relate their effective mechanical properties to specific aspects of the fabric morphology and microstructure.

Theoretical investigations to develop relationships between the various parameters which characterize a woven fabric have ranged from the purely geometrical model of Peirce [1] to the more physical mechanistic models of Olofsson [2] and Grosberg and Kedia [3]. A summary of the analysis of the mechanical properties of woven fabric prior to 1969 is included in the monograph by Hearle et al. [4], and more recent summaries have been provided by Ellis [5] and Treloar [6]. The mechanistic approaches have traditionally uncoupled the effects of yarn stretching from the effects of yarn bending (crimp interchange effect). The bending effects are obtained by modeling the yarns as inextensible elastica, and these bending deformations are superimposed unto the stretching deformations to obtain the total elastic response. This uncoupled approach provides estimates of a much stiffer mechanical response of the woven fabric than is observed experimentally. Recently, Warren [7] has provided an analysis of woven fabric which models the individual yarns as "extensible" elastica and thus couples bending and stretching effects throughout the deformation history. Following a general development of the nonlinear theory, Warren [7] restricts interest to small deformations and loads and obtains explicit representations for the in-plane linear elastic constants of the fabric in terms of the initial weave geometry and the elastic properties of the individual yarns. Even for these linear elastic results, the coupling between bending and stretching effects is complex

and not well represented by simple superposition. The results of this linear analysis provide estimates for the in-plane elastic constants which agree very well with results obtained experimentally by Leaf and Kandil [8] on fabrics woven from Vincel rayon yarns.

In this work we extend our previous results [7] to provide a theoretical investigation of the large deformation elastic response of a plane woven Kevlar fabric together with a comparison of these theoretical results with experimental data obtained from uniaxially loaded Kevlar fabrics. We define the woven fabric as a regular network of orthogonal interlaced yarns and denote a point on any yarn which is midway between successive cross yarns as a yarn midpoint. For homogeneous deformations of this woven fabric we may restrict our analysis to the yarn deformations which occur between two adjacent yarn midpoints. We model the individual yarns as extensible elastica, thus coupling stretching and bending effects at the outset. Consideration is restricted to biaxial loading in the principal yarn directions in the plane of the fabric. The initial unloaded yarn geometry is assumed to be a sequence of alternating circular arcs of constant radius R as apparently considered first by Olofsson [9]. We utilize the general results obtained in [7] to investigate the asymptotic elastic behavior for large applied loads. Interestingly enough, the limiting results of this asymptotic analysis for small applied forces provide a very close approximation to the linear elastic response obtained in [7].

We first obtain the solution to the differential equation describing the nonlinear deformation of an extensible elastica subjected to a normal contact force $2V$ and a midpoint force T_o. This provides the deflection-force relations for the individual yarns. The mechanical response of the woven fabric is obtained from the interaction of two of these solutions corresponding to the yarn overlap by enforcing equilibrium and compatibility of displacements. This provides analytical expressions for the in-plane displacement-force relations of the woven fabric in the two principal yarn directions.

Deflection-force relations for a fabric woven from 400 denier Kevlar yarns has been determined experimentally under conditions of uniaxial loading. Specimens were tested in both warp and fill directions, and the deflection-force relations obtained experimentally are in quite good agreement with the theoretical predictions. During initial loading the elastic response of the fabric is dominated by yarn bending. With increased loading the response goes through a transition from bending to stretching and for large loads is dominated by yarn stretching. The difference between bending and stretching effects is significant and this difference is reflected in both the experimental and theoretical results. This particular fabric is found to be stiffer in the fill direction than in the warp which is consistent with the initial weave geometry showing the yarn crimp height greater for the warp yarns than the fill. This increased crimp height requires more bending deformation to straighten out the warp yarns, and this difference is captured in both the theoretical and experimental results.

ANALYSIS OF INDIVIDUAL YARNS

The first step in obtaining the displacement-force relations for the woven fabric is to obtain displacement-force relations for the individual yarns. In this analysis, each yarn is modeled as an extensible elastica, and the geometry of this model is shown in Fig.1 where we have made use of symmetry about the z-axis corresponding to the yarn overlap contact point. The extensible elastica has been considered in detail by Antman [10] and Tadjbakhsh [11], and in this analysis we make use of the intrinsic coordinates of the elastica as presented for the inextensible case by Mitchell [12]. The elastica is assumed to deform in the (x,z) plane as shown, and the initial shape is taken to be an arc of a circle of radius R subtending an angle ϕ_o. The undeformed shape of the elastica is defined by the arc length s_o, $0 \le s_o \le L_o$, and the slope $\phi(s_o) = s_o/R$. The deformed shape is defined by the arc length s, $0 \le s \le L$, and slope $\psi(s)$.

The elastica is assumed to stretch linearly under the effect of the axial force T(s) acting through the centroid of the cross section of area A which provides

$$\frac{ds}{ds_0} = 1 + \frac{T(s)}{EA} , \qquad (1)$$

where E is the Young's modulus of the elastica, and

$$T(s) = F\cos\psi + V\sin\psi = T_0 \cos(\psi - \alpha) .$$

A number of synthetic yarns exhibit yielding and the linear relation of (1) is valid only for T(s) less than the yarn yield force. Yarns woven from Kevlar fibers, however, show an essentially linear displacement-force relation for loads up to fracture, and for these yarns Eqn. (1) is valid for the entire loading history. We note that the antisymmetric condition at the deformed yarn midpoint s=L, with slope $\psi = \psi_0$, requires the bending moment M(s) to vanish at this point.

The differential equation which describes the non-linear deformation of the extensible elastica together with the appropriate boundary conditions for this problem have been developed by Warren[7] and all the details of this development will not be reproduced here. Our point of departure is a first integral of this differential equation as presented in [7] which takes the form

$$R\left[1 + \kappa R^2\gamma \cos(\psi-\alpha)\right]\frac{d\psi}{ds} = \left\{1 + 2\kappa R^2\left[\cos(\psi_0-\alpha)-\cos(\psi-\alpha)\right] + \kappa^2R^4\gamma\left[\cos^2(\psi_0-\alpha)-\cos^2(\psi-\alpha)\right]\right\}^{1/2} \qquad (2)$$

and we have made use of the two constants

$$\kappa = \frac{T_0}{EI} , \qquad \gamma = \frac{I}{AR^2} , \qquad (3)$$

where I is the effective moment of inertia of the yarn cross-section. The constant γ represents a measure of the relative effects of bending and stretching in the

deformation of the elastica with the case $\gamma=0$ representing the inextensible elastica. The differential equation (2) is subject to the boundary condition

$$\psi(0) = 0 . \tag{4}$$

Equation (1) provides the relation between ds and ds_0 of

$$ds = \left[1 + \kappa R^2 \gamma \cos(\psi-\alpha)\right] ds_0 , \tag{5}$$

which is important in evaluating the deformed slope ψ_0 at the end s=L. We note that the differential equation (2) may be expressed as an elliptic integral of Weirstrass' form [10], but this does not provide an explicit representation for the unknown ψ_0 in terms of the known parameters. In reference [7], approximate solutions of (2) were obtained for small applied forces such that $\kappa R^2 << 1$.

We now consider approximate solutions of Eqn. (2) for the specific situations where ψ_0 and α are small which occur under conditions of loose weave geometry or for large in-plane forces $F = f_x$. Formally, we assume now that $\psi_0^2 << 1$, $\alpha^2 << 1$, which implies that $V/F = \tan\alpha = \alpha$. We define the dimensionless forces associated with $F = f_x$ and V as

$$\begin{aligned} \hat{f}_x &= \kappa R^2 \cos\alpha = \kappa R^2 , \\ \hat{V} &= \kappa R^2 \sin\alpha = \alpha\kappa R^2 = \alpha \hat{f}_x . \end{aligned} \tag{6}$$

From Eqns. (2) and (5), the undeformed increment of arc length ds_0 is given by

$$\sqrt{K}\,\frac{ds_0}{R} = \frac{d\psi}{\sqrt{\Omega(\psi)}} , \tag{7}$$

where

$$K = \hat{f}_x(1 + \gamma \hat{f}_x) , \tag{8}$$

and

$$\Omega(\psi) = (\psi_0-\psi)^2 + 2(\alpha-\psi_0)(\psi_0-\psi) + 1/K \ . \qquad (9)$$

Integration of Eqn. (7) gives

$$\sqrt{K}\ \phi_0 = \int_0^{\psi_0} \frac{d\psi}{\sqrt{\Omega(\psi)}} \ ,$$

and evaluation finally provides

$$\psi_o = \frac{1}{\sqrt{K}} \frac{(1-m^2)}{(1+m^2)} + \alpha \frac{(1-m)^2}{(1+m^2)} \ , \qquad (10)$$

with

$$m = e^{-\sqrt{K}\phi_o} \ . \qquad (11)$$

Equation (10) determines the yarn midpoint slope ψ_o as a function of the initial yarn geometry ϕ_o and the applied forces. For large values of applied force, $K \rightarrow \infty$, $m \rightarrow 0$, and $\psi_o \rightarrow \alpha$.

The deformed increment of arc length ds may be obtained from Eqn. (2) and is given by

$$\sqrt{K}\ \frac{ds}{R} = \left\{1 + \gamma \hat{f}_x \left[1 - \frac{1}{2}(\psi-\alpha)^2\right]\right\} \frac{d\psi}{\sqrt{\Omega(\psi)}} \ . \qquad (12)$$

Using the deformed geometry relations $dx = \cos\psi\, ds$ and $dz = \sin\psi\, ds$ together with Eqn. (12), the position of the deformed yarn midpoint (x_o , z_o) may be obtained in terms of the deformed yarn midpoint slope ψ_o through direct integration, with ψ_o given by Eqn. (10). Carrying out these operations provides expressions for the deformed position of the yarn midpoint in terms of the initial yarn geometry and the applied forces. The components of the deformed position are given by

$$\frac{x_0}{R} = (1+\gamma \hat{f}_x)\,\phi_0 - \frac{1}{2}\alpha^2\phi_0 - \frac{1}{4K}(1+2\gamma\hat{f}_x)\left[\frac{\alpha(1-m)^2}{(1+m^2)} + \frac{(1-m^2)}{\sqrt{K}(1+m^2)}\right]$$

$$+ \frac{\alpha}{4\sqrt{K}}(3+2\gamma\hat{f}_x)\left[\frac{\alpha(1-m^2)}{(1+m^2)} - \frac{(1-m)^2}{\sqrt{K}(1+m^2)}\right] \qquad (13)$$

$$+ (1+2\gamma\hat{f}_x)\,\phi_0\left[\left(\frac{1}{K}-\alpha^2\right)\frac{m^2}{(1+m^2)^2} + \frac{\alpha\, m\,(1-m^2)}{\sqrt{K}(1+m^2)}\right],$$

$$\frac{z_0}{R} = (1+\gamma\hat{f}_x)\left[\alpha\phi_0 - \frac{\alpha(1-m^2)}{\sqrt{K}(1+m^2)} + \frac{(1-m)^2}{K(1+m^2)}\right]. \qquad (14)$$

It is instructive to consider two limiting cases of these results.

(i) Limit as $f_x \to \infty$ and $V \to \infty$

Within the framework of this analysis, as $f_x \to \infty$ and $V \to \infty$, the ratio $V/f_x = \alpha << 1$. Equation (10) shows that under these conditions, $\psi_0 \to \alpha$ and the deformed position of the yarn midpoint has the components

$$x_0 = \frac{L_0 f_x}{EA}, \qquad z_0 = \frac{L_0 V}{EA}.$$

Thus in the limit of large f_x, V, the yarn straightens out and the elastic response approaches that of a straight rod oriented at $\psi_0 = \alpha = V/f_x$.

(ii) Limit as $f_x \to 0$ and $V \to 0$

This limiting case provides the linear elastic response of the yarn, and Eqns. (10), (13), and (14) provide

$$\psi_0 = \phi_0 - \frac{1}{3}\phi_0^3 \hat{f}_x + \frac{1}{2}\phi_0^2 \hat{V} ,$$

$$\frac{x_0}{R} = (\phi_0 - \frac{1}{6}\phi_0^3) + \left[\gamma(\phi_0 - \frac{1}{3}\phi_0^3) + \frac{2}{15}\phi_0^5\right]\hat{f}_x - \frac{1}{4}\left[-2\gamma\phi_0^2 + \frac{5}{6}\phi_0^4\right]\hat{V} , \qquad (15)$$

$$\frac{z_0}{R} = \frac{1}{2}\phi_0^2 - \frac{1}{4}\left[-2\gamma\phi_0^2 + \frac{5}{6}\phi_0^4\right]\hat{f}_x + \frac{1}{3}\phi_0^3 \hat{V} .$$

These results agree with the linear elastic response developed in [7] through the appropriate order of the initial geometry parameter ϕ_0. It is interesting to note that while the results of this analysis were obtained with the assumption of small α and large f_x, they provide a very accurate representation of the yarn response for the linear elastic limit. A measure of the error between the actual linear elastic response and the linear response represented by Eqn. (15) may be obtained by considering the exact initial yarn geometry $(x_0/R)_0 = \sin\phi_0$ and $(z_0/R)_0 = (1-\cos\phi_0)$. Even for fairly tight weaves with $\phi_0 = 45^o$, the error in $(x_0/R)_0$ is less than one percent and the error in $(z_0/R)_0$ is about five percent.

The displacement of the yarn midpoint with respect to the overlapping yarn contact point (0,0) is the difference between the deformed and undeformed positions of the yarn midpoint. This displacement has components u_x and u_z which may be obtained in the dimensionless form

$$\hat{u}_x = \frac{u_x}{R} = \frac{x_0}{R} - (\phi_0 - \frac{1}{6}\phi_0^3) ,$$

$$\hat{u}_z = \frac{u_z}{R} = \frac{z_0}{R} - \frac{1}{2}\phi_0^2 , \qquad (16)$$

where x_0/R is given by Eqn. (13), z_0/R is given by Eqn. (14), and we have used the approximate undeformed yarn midpoint position given in Eqn. (15). Equation (16) provides the displacement-force relations for the individual yarns.

ANALYSIS OF WOVEN FABRIC

The interlaced geometry of a typical woven fabric is shown in Fig. 2. With reference to Fig. 2b, the usual geometrical weave parameters of pick spacing p, yarn length ℓ and crimp height h are represented in terms of the elastica parameters R and ϕ_o by

$$p = 2R \sin \phi_o$$

$$\ell = 2R\phi_o \qquad (17)$$

$$h = 2R (1 - \cos \phi_o) .$$

To fix ideas, we will denote the x-direction as the warp direction and the y-direction as the weft or fill direction.

The large deformation elastic response of a woven fabric which is loaded biaxially with forces f_x and f_y in the plane of the fabric may be determined directly from the displacement-force relations of Eqn. (16). The warp yarns in the (x,z) plane will exhibit displacements u_x and u_{zx} which depend on the initial warp yarn geometry, the elastic properties of the warp yarns, and the forces f_x and V. In a similar manner, the fill yarns in the (y,z) plane will exhibit displacements u_y and u_{zy} which depend on the initial fill yarn geometry, the elastic properties of the fill yarn, and the forces f_y and V. In these relations we have made use of the fact that equilibrium in the z-direction at the warp and fill yarn contact point requires the contact force V to be the same for both yarns. The yarns are assumed to remain in contact during deformation, and recognizing that one yarn will be concaved downward while the other is concaved upward provides the displacement compatibility condition

$$u_{zx} + u_{zy} = 0 . \qquad (18)$$

Equations (14) and (16) show that the transverse displacements u_{zx} and u_{zy} depend linearly on the angle α and therefore depend linearly on the contact force V.

Thus the compatibility condition (18) provides a straightforward representation of the contact force V as a function of f_x and f_y and the geometric and material properties of the warp and fill yarns. With $V(f_x, f_y)$ known, the ratios $V/f_x = \alpha_x$ and $V/f_y = \alpha_y$ associated with the warp and fill yarns, respectively, may be defined. Then for any combination of biaxial loads in the plane of the weave, the in-plane displacements $u_x(f_x, f_y)$ and $u_y(f_x, f_y)$ may be evaluated from Eqn. (16_1) with (13). We will not present the results for biaxially loaded fabrics since our main interest here is on a comparison of this theory with experiments performed on woven Kevlar fabrics loaded uniaxially in tension. Theoretical results for the elastic deformation of fabrics subjected to uniaxial loading are developed in the next section.

RESULTS FOR UNIAXIAL LOADING

In this section we obtain the displacement-force relations for a woven fabric subjected to uniaxial loading in a principle direction parallel to one of the yarns. Without loss of generality, we take the direction of loading to be in the warp or x-direction and this yarn is subjected to the forces f_x and V. The fill or y-directed yarn is unloaded in the plane, so $f_y = 0$ and this yarn is subjected to the transverse force V only. Thus for the fill yarn, $\alpha_y = \pi/2$ and the analysis developed for $\alpha^2 << 1$ is not appropriate. In this analysis, a subscript x or y will denote properties associated with the x or y directed yarn and these subscripts are used only when necessary to differentiate between the two. Absence of a subscript implies properties of the warp or x-directed yarn.

We assume that the displacement of the fill yarn depends linearly on the contact force V, and that with $f_y = 0$ there will be negligible stretching of the fill yarn. Thus for this inextensible fill yarn we take the stretching parameter $\gamma_y = 0$, and the linear

analysis of [7] provides (Eqn. (27) of [7])

$$u_y = - \frac{R_y^3 B_y}{4E_y I_y} V \ , \qquad u_{zy} = \frac{R_y^3 C_y}{4E_y I_y} V \ , \tag{19}$$

with B_y, C_y approximated by

$$B_y = \frac{5}{6} \phi_{0y}^4 \left(1 - \frac{1}{3} \phi_{0y}^2\right) \ , \qquad C_y = \frac{4}{3} \phi_{0y}^3 \left(1 - \frac{9}{20} \phi_{0y}^2\right) \ . \tag{20}$$

The approximations of Eqn. (20) are within 1% of the exact expressions given in [7] for the geometries under consideration here. The compatibility condition (18) provides

$$\alpha = \frac{V}{f_x} = \frac{\left\{\frac{1}{2}\phi_0^2 - \frac{1\ (1-m)^2}{\hat{f}_x\,(1+m^2)}\right\}}{\left\{(1+\gamma\hat{f}_x)\phi_0 + \frac{1}{3}N\hat{f}_x\phi_0^3 - \frac{\sqrt{K}\,(1-m^2)}{\hat{f}_x\,(1+m^2)}\right\}} \ , \tag{21}$$

with

$$N = \left(\frac{E_x I_x}{E_y I_y}\right)\left(\frac{R_y \phi_{0y}}{R_x \phi_{0x}}\right)^3 \left(1 - \frac{9}{20}\phi_{0y}^2\right) \ . \tag{22}$$

The dimensionless warp displacement u_x from Eqn. (16_1) with (13) is given by

$$\begin{aligned} \hat{u}_x = {} & \gamma \hat{f}_x \phi_0 - \frac{1}{2}\alpha^2 \phi_0 + \frac{1}{6}\phi_0^3 - \frac{(1+2\gamma\hat{f}_x)}{4K}\left[\frac{\alpha\,(1-m)^2}{(1+m^2)} + \frac{(1-m^2)}{\sqrt{K}\,(1+m^2)}\right] \\ & + (1+2\gamma\hat{f}_x)\,\phi_0\left[\left(\frac{1}{K} - \alpha^2\right)\frac{m^2}{(1+m^2)^2} + \frac{\alpha\, m\,(1-m^2)}{\sqrt{K}\,(1+m^2)^2}\right] \\ & + \frac{\alpha}{4\sqrt{K}}(3+2\gamma\hat{f}_x)\left[\frac{\alpha\,(1-m^2)}{(1+m^2)} - \frac{(1-m)^2}{\sqrt{K}\,(1+m^2)}\right] \ , \end{aligned} \tag{23}$$

with α given by Eqn. (21). For a particular plane woven fabric with pick spacings p_x, p_y, crimp heights h_x, h_y, or known yarn lengths ℓ_x, ℓ_y, the geometric parameters R_x, ϕ_{ox} and R_y, ϕ_{oy} are determined from Eqns. (17) and the warp displacement u_x evaluated for a uniaxial load f_x as shown. Clearly the x and y directions for this fabric may be interchanged to provide the displacement u_y for a uniaxial load f_y.

COMPARISON WITH EXPERIMENT

The deflection-force relations of a plane fabric woven from 400 denier Kevlar yarns have been determined experimentally as part of a parachute fabric investigation at Sandia National Laboratories. This particular fabric has nominally 30 yarns per inch in the warp direction and 31 yarns per inch in the weft or fill direction. One inch wide specimens were cut from this fabric and were sufficiently long to provide a 10 inch gage length when installed in an Instron testing machine. Specimens were cut in both the warp and fill directions, and care was taken to insure 30 yarns in the warp direction and 31 yarns in the fill. In these experiments, a specimen cut from, say, the warp direction, was installed in the Instron and loaded uniaxially to a given level while the deflection-force relation was recorded, and the loading stopped. A mold was fitted about the specimen and a portion of the specimen encapsulated. The specimen was then unloaded and removed from the Instron, sectioned in both warp and fill directions, and photographed. A second specimen cut in the warp direction was then installed in the Instron, loaded to a higher level than the first with deflection-force data recorded, and the loading stopped. Encapsulation, unloading, sectioning, and photographing was repeated at this higher load level. Altogether, this process was repeated at four load levels for specimens cut in both warp and fill directions to reveal the changes in weave geometry and yarn cross-section with loading. An unloaded specimen was also encapsulated, sectioned, and photographed to obtain the initial weave geometry. The

deflection-force records were remarkably consistent within the different load levels. A detailed summary and discussion of the results of these experiments, including results obtained on fabrics woven from 200 denier Kevlar yarns, is in preparation [13].

Our main interest here is in comparing deflection-force relations obtained from these experiments on a uniaxially loaded fabric with the theory just developed. We again denote the fabric warp direction as the x-axis and the fabric fill direction as the y-axis. The initial geometry of the yarns in these directions as obtained from the sectioned photographs of the the unloaded fabric are listed in Table 1. The measured pick space p and crimp height h represent average values through the section while the parameters R and ϕ_o are derived from these average values using Eqn. (17). The measured pick spacings differ by about 2% from the nominal values. Also shown in Table 1 are the effective elastic properties EA and I/A of each yarn. The effective yarn stretching stiffness EA was obtained from averaged displacement data for large forces in both warp and fill directions, and the I/A values were obtained from curve fitting appropriate values of γ at the lower load levels with Eqn. (3_2). These values indicate that there is essentially no difference between the elastic properties of the warp and fill yarns for this particular fabric.

The experimental and theoretical deflection-force relations for loading in the warp and fill directions are shown and compared in Figures 3 and 4. We have denoted the true displacement of the specimen measured over the ten inch gage length by $\bar{u}$ and the true or total force applied to the one inch wide specimen by $\bar{f}$. In terms of the dimensionless displacements of Eqn. (16) and the dimensionless forces of Eqn. (6), the $\bar{u}$ and $\bar{f}$ are given by

$$\bar{u}_x = 508 \left(\frac{R_x}{p_x} \right) \hat{u}_x \quad \text{mm} ,$$

$$\bar{f}_x = 4.448 \left(\frac{E_x I_x}{R_x^2 p_y} \right) \hat{f}_x \quad \text{N} . \tag{24}$$

These flexible specimens are difficult to install in the Instron grips and there is some uncertainty as to the actual origin in all of the experimental ($\bar{u}$, $\bar{f}$) curves. We have circumvented this problem by positioning the curves along the u axis so as to line up with each other in the large load limit.

Figures 3 and 4 show quite good agreement between experiment and theory in both warp and fill direction. During initial loading the elastic response of the fabric is dominated by yarn bending. With increased loading the response goes through a transition from bending to stretching and for large loads is dominated by yarn stretching. The difference between bending and stretching effects is significant. For small values of force $\bar{f}_x$, $\bar{f}_y$, Eqn. (15) shows

$$\bar{u}_x = 7.42 \times 10^{-2} \bar{f}_x , \qquad \bar{u}_y = 4.60 \times 10^{-2} \bar{f}_y , \tag{25}$$

while for large values of force

$$\Lambda\bar{u}_x = 3.81 \times 10^{-3} \Lambda\bar{f}_x , \qquad \Lambda\bar{u}_y = 3.77 \times 10^{-3} \Lambda\bar{f}_y . \tag{26}$$

Thus in the warp direction the elastic compliance changes by a factor of 20 and in the fill direction by a factor of 12. These results show that overall the fabric is stiffer in the fill direction than in the warp. This is consistent with the initial weave geometry presented in Table 1 where the crimp height h is greater for the warp yarns than for the fill which provides a larger angle ϕ_o for the warp yarns. This difference probably

came about because of warp displacement during shedding and differences in yarn tension during weaving. Under loading in the fabric plane, more bending deformation is required to straighten out the warp yarns, and this difference in deformation is reflected in Eqn. (24) and in Figures 3 and 4. It appears from this comparison of experiment with theory that the deformation of plane woven Kevlar fabric can be quite accurately predicted by modeling the individual yarns as extensible elastica.

REFERENCES

1. Peirce, F. T. , "The Geometry of Cloth Structures", J. Text. Inst. , 28 (1937) T45.
2. Olofsson, B. , "A General Model of a Fabric as a Geometric-Mechanical Structure", J. Text. Inst. , 55 (1964) T541.
3. Grosberg, P. and Kedia, S., "The Mechanical Properties of Woven Fabrics, Part I: The Initial Load Extension Modulus of Woven Fabrics", Textile Res. J., 36 (1966) 71.
4. Hearle, J. W. S., Grosberg, P., and Backer, S., Structural Mechanics of Fibers, Yarns, and Fabrics, Wiley-Interscience, NY (1969).
5. Ellis, P., "Woven Fabric Geometry -- Past and Present", Tex. Inst. & Industry, 12 (1974) 245.
6. Treloar, L. R. G., "Physics of Textiles", Physics Today, 30 (1977) 23.
7. Warren, W. E., "The Elastic Properties of Woven Polymeric Fabric", Poly. Eng. & Science , 30 (1990) 1309.
8. Leaf, G. A. V. and Kandil, K. H., "The Initial Load-Extension Behavior of Plane-Woven Fabrics", J. Text. Inst., 71 (1980) 1.
9. Olofsson, B., "The Setting of Wool Fabrics-- A Theoretical Study", J. Text. Inst., 52 (1961) T272.
10. Antman, S., "General Solutions for Plane Extensible Elasticae having Nonlinear Stress-Strain Laws", Q. Appl. Math. , 26 (1968) 35.
11. Tadjbakhsh, I., "The Variational Theory of the Plane Motion of the Extensible Elastica", Int. J. Engng. Sci. , 4 (1966) 433.
12. Mitchell, T. P., "The Nonlinear Bending of Thin Rods", J. Appl. Mech. , 26 (1959) 40.
13. Ericksen, R. H., Davis, A. C., and Warren, W. E., "Deflection-Force Measurements and Observations on Kevlar 29 Parachute Fabrics", in preparation.

FIGURE CAPTIONS

Figure 1. The extensible elastica: (a) Schematic of woven yarn, (b) The intrinsic coordinates and applied forces, (c) Forces acting on an element.

Figure 2. Geometry of the woven fabric: (a) Schematic of woven yarn interlace, (b) Cross-section of weave in either x (warp) or y (fill) direction.

Figure 3. Displacement-force relations for uniaxial loading in the x (warp) direction. Solid line is experimental, broken line is theory, – • – • – • – is linear [7].

Figure 4. Displacement-force relations for uniaxial loading in the y (fill) direction. Solid line is experimental, broken line is theory, – • – • – • – is linear [7].

Table 1. Initial weave geometry and elastic properties

	p (mm)	h (mm)	R (mm)	ϕ_o (rad)	EA (N)	I/A (mm^2)
x (warp)	0.805	0.113	1.460	0.279	2200	4.90×10^{-5}
y (weft)	0.829	0.092	1.885	0.222	2160	4.97×10^{-5}

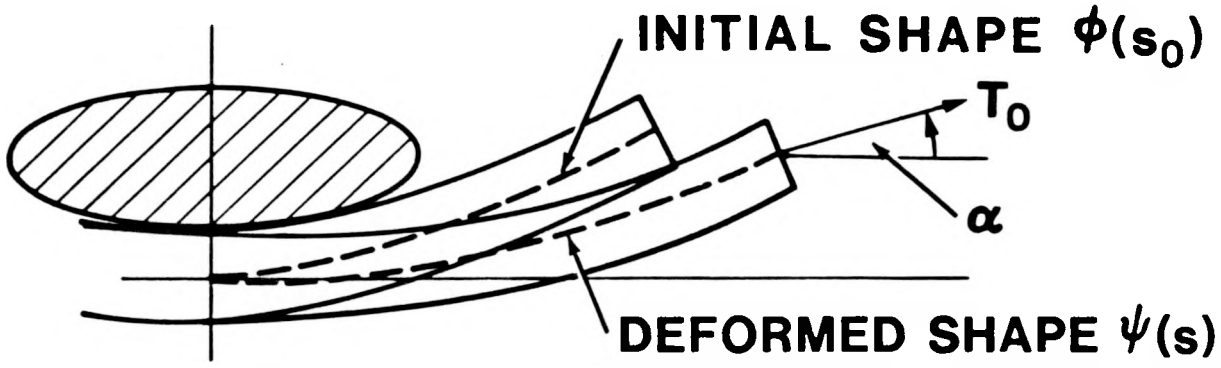
INITIAL SHAPE $\phi(s_0)$
T_0
α
DEFORMED SHAPE $\psi(s)$

(a)

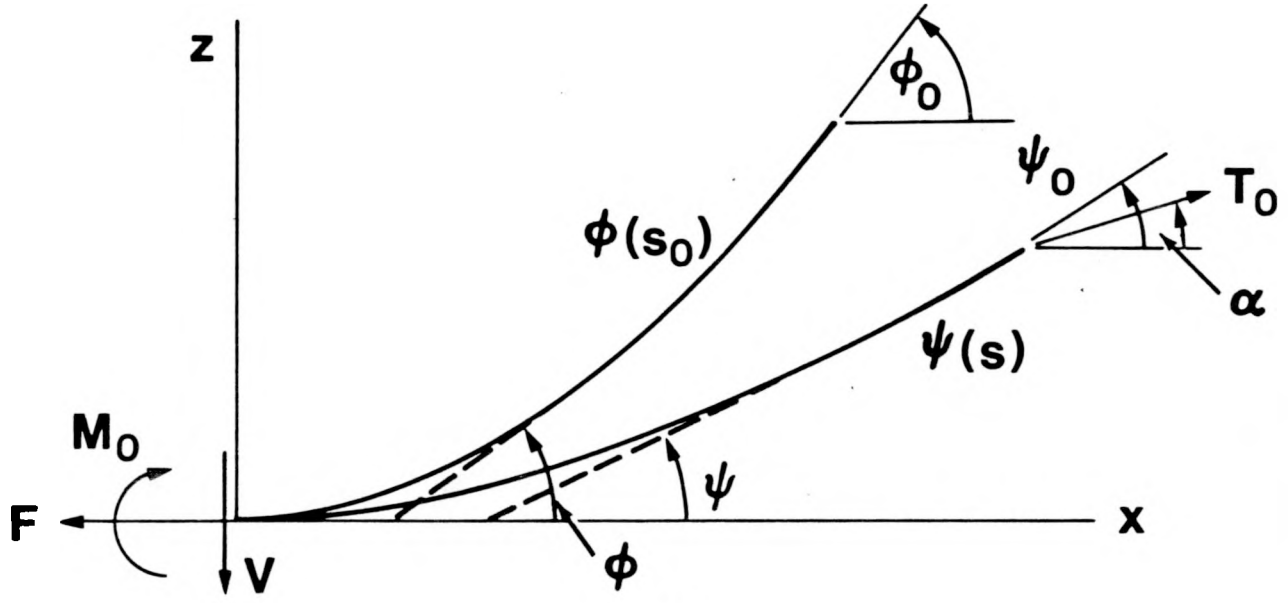
z
ϕ_0
ψ_0
T_0
$\phi(s_0)$
α
$\psi(s)$
M_0
F
V
ψ
ϕ
x

(b)

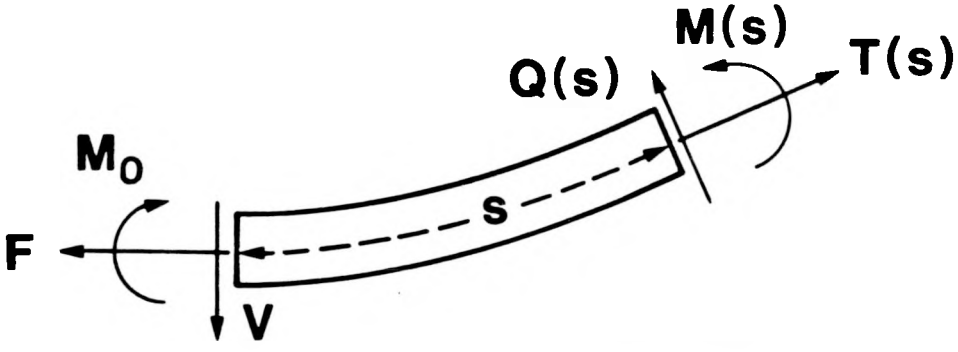
M(s)
Q(s)
T(s)
M_0
s
F
V

(c)

Fig. 1

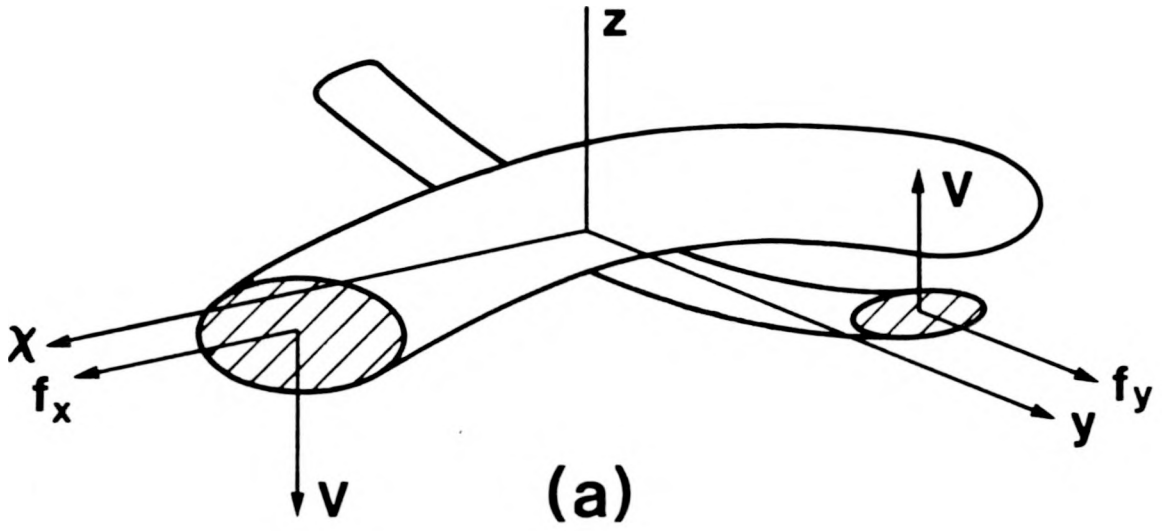

(a)

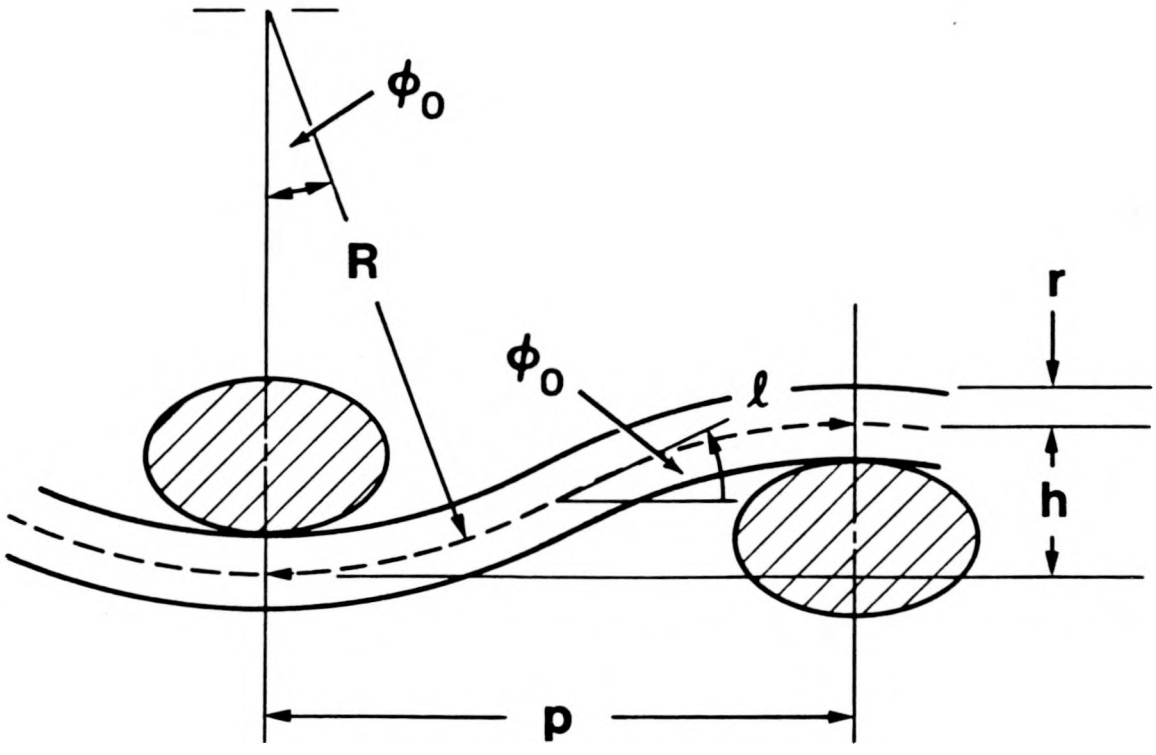

(b)

Fig. 2

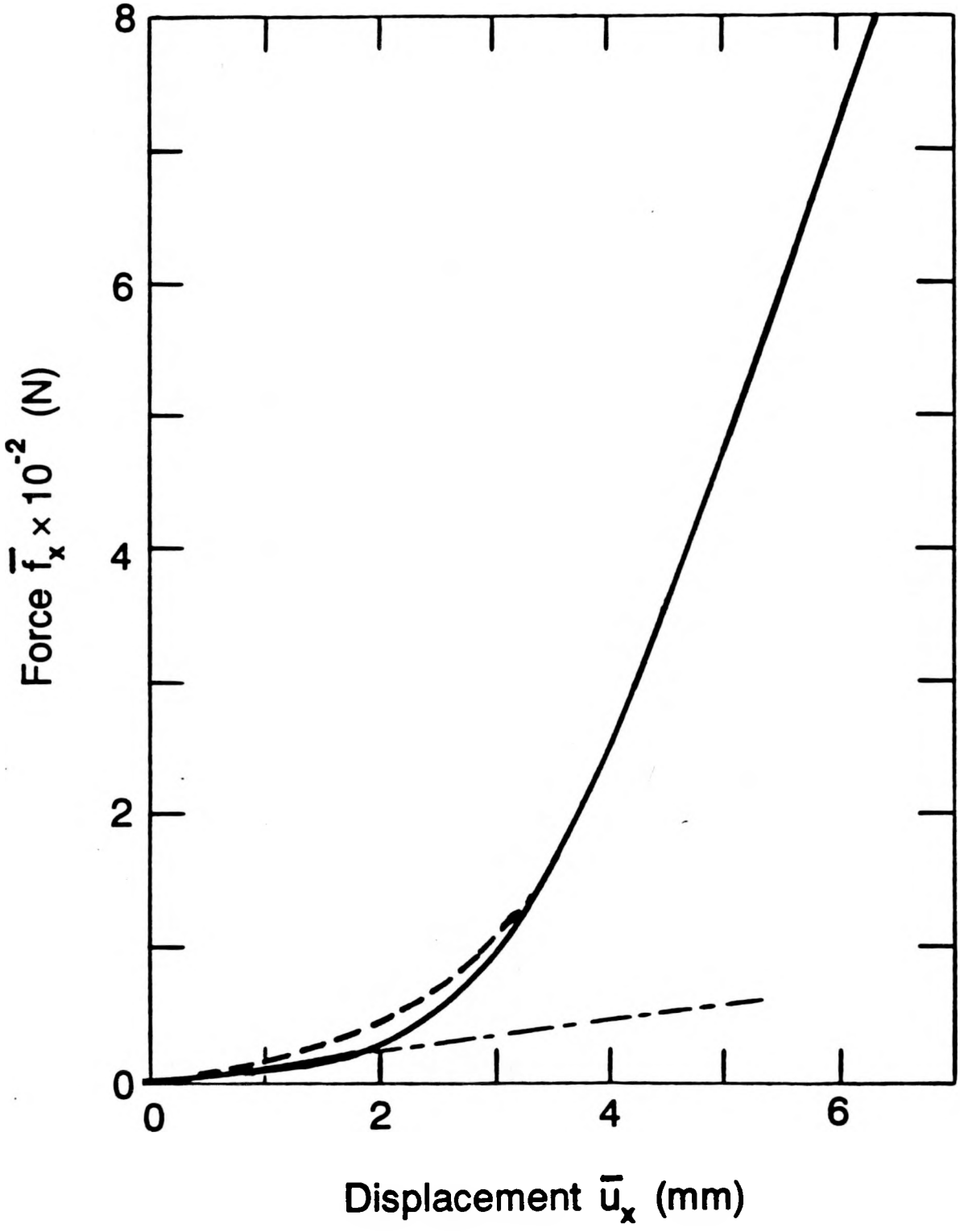

Fig. 3

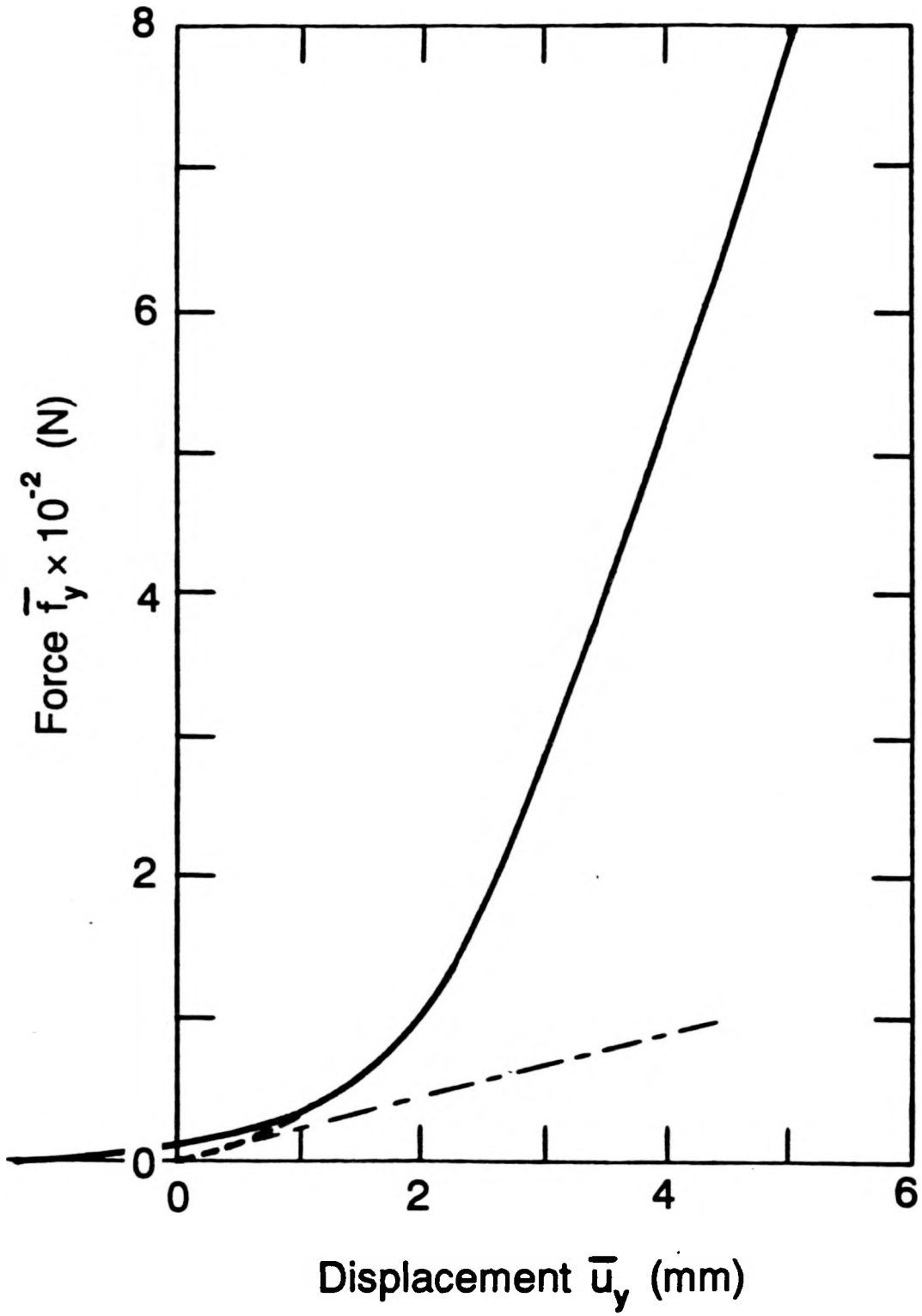

Fig. 4